NMR crystallography: the use of dipolar interactions in polymorph and co-crystal investigation

UNIVERSITÀ DEGLI STUDI DI TORINO

NMR CRYSTALLOGRAPHY: THE USE OF DIPOLAR INTERACTION IN POLYMORPH AND CO-CRYSTAL INVESTIGATION

Michele R. Chierotti and Roberto Gobetto

Received (in XXX, XXX) Xth XXXXXXXXX 20XX, Accepted Xth XXXXXXXXX 20XX
DOI: 10.1039/b000000x

Abstract

The use of dipolar interaction in solid-state NMR spectroscopy represents a powerful tool to access information on chemical structure at molecular level on solid compounds and materials. The study of polymorphs and co-crystals is one of the more active research field where the possibilities offered by the new emerging NMR crystallography reveal all their potential. The aim of this article is to offer the state-of-the-art on this subject in order to develop new insights and to promote cooperative efforts in the fascinating field of polymorphs and co-crystals.

CV and picture of Michele R. Chierotti

Michele R. Chierotti graduated at the University of Torino (2002). In 2006, he received his PhD in Chemistry in the same University after a period at Durham University (Prof. R.K. Harris). Since 2010 he is permanent researcher at the University of Torino. His scientific activity, focused on design, synthesis and characterization (mainly by solid-state NMR) of organic and organometallic crystal forms, is documented by more than 50 ISI-listed scientific publications.

CV and picture of Roberto Gobetto
Roberto Gobetto born in 1956 won a researcher position in 1983 at the University of Torino where he is currently full professor of Inorganic Chemistry since 2000. He has served as visiting professor at the University of Northridge (USA) and at University of Durham (UK). His main research interests, focused on solid-state NMR, organometallic luminescent probes and hyperpolarization, are documented by more than 240 papers on international journals.

.

Introduction

The isolation, identification and characterization of different crystal forms of the same molecule (polymorph or pseudo-polymorphs) or of aggregates of the same molecule with other molecules (co-crystals) represent one of the most active areas of the modern solid-state chemistry. This field, called crystal engineering, has evolved in recent years gaining a special interest not only in academia but also in many applicative areas.[1] Crystal engineering aims at designing and synthesizing functional materials from molecular and ionic building blocks in a "bottom-up" process. With a supramolecular approach, it involves modifications of the crystal packing of a solid material by changing the internal arrangement of the molecules through establishing of non-covalent bonds (e.g., hydrogen bonding, van der Waals forces, π-stacking, electrostatic interactions).

Thus, the expansion of crystal engineering during the last few years has gone parallel with a significant interest in the origin and nature of intermolecular weak interactions and their use in the design and preparation of new crystal forms. Indeed, a sharp use of these contacts allows modulating physical and chemical properties of the component of interest without compromising its chemical integrity. Usually, solid-state researchers take advantage of many different strategies when trying to modify the chemical and physical solid-state properties of a target molecule. Recently, particular attentions have been devoted to the formation of polymorphs, hydrates, solvates, salts and co-crystals.[2]

Nevertheless, there is a need for a better comprehension of the structure-property correlations that can be reached only by the understanding of the structural behaviors of the new crystal forms. This makes X-ray diffraction techniques the preferred method for the characterization of the products since it provides the final 3D structure. In this context, NMR crystallography is an emerging discipline which, supporting the diffraction techniques, is growing accepted also in the crystal engineering field. In particular, when dealing with hydrogen atom positions or with microcrystalline or partially ordered samples, which are all rather difficult to investigate via the standard diffraction methods, the problem can be tackled in two ways: a) by using microcrystals to "seed" a solution and to obtain single crystals of the new form for a conventional crystal structure determination; b) by employing NMR crystallography which combines the complementary techniques of solid-state NMR (SSNMR), powder diffraction and computational methods. Indeed, while diffraction experiments reveal long order data, SSNMR unravels number of independent molecules and their symmetry, proximities and distances, connections and orientation relations, namely all information on local and intermediate length scales. Molecular modeling and quantum chemical simulations complete/support the characterization and help to create meaningful model structures.[3] This approach has been proved successful for a broad variety of materials also taking advantage of new generation SSNMR spectrometers and new pulse sequences.[4] The combination of techniques plays a significant role in structural solution both at solid as well as for low molecular gels and soft materials where the crystallization is not possible as the molecules tend to form gels as recently reported.[5]

Thanks to a multinuclear and multiparametric approach, SSNMR can really speed up and increase the reliability of the XRPD structure determinations. Among all NMR parameters chemical shift, chemical shielding tensors, dipolar interaction, spin diffusion,

and nuclear quadrupole coupling are the most important and have been reviewed in a book which is already a cornerstone of this discipline.[6]

While the use of the chemical shift has been extensively reviewed by R.K. Harris[7] the focus of this trend article is to highlight recent application of the dipolar interaction, both homo- and heteronuclear, in the evaluation of proton-proton and proton-carbon or proton-nitrogen connectivities. Indeed, owing to its dependence to the atom distance ($D \propto r^{-3}$), it represents the parameter with the highest crystallographic content. Special emphasis will be given to polymorphs, salts and co-crystals while for a comprehensive overview of other fields we suggest ref. 6. A small initial part will be also dedicated to a brief revision of the NMR pulse sequences used for extracting information on the dipolar coupling.

Dipolar interaction and SSNMR sequences

The last two decades have witnessed a sharp rise in the application of SSNMR in the investigation of crystalline and amorphous solids. The technique is particularly appealing for cases that cannot be studied by X-ray diffraction and has been extensively employed to investigate reaction intermediates,[8] membrane proteins,[9] pharmaceutical molecules,[10] new inorganic,[11] organic and hybrid materials.[12] For a complete investigation it is often necessary to associate to the SSNMR data the complementary use of IR and Raman spectroscopies and differential scanning calorimetry (DSC). Combination of SSNMR methods with XRPD data can be successfully applied toward a complete crystal structure determination.[13]

Different chemical environments of the nuclei with non-null spin are detected by SSNMR allowing the use of several "nuclear probes" to get information on structure and dynamics of the solid under investigation. Local environment affects obviously the chemical shift, but, if one considers that this parameter is a second-rank tensor, new structural information can be obtained by the evaluation of the chemical shift principal values from spinning sideband manifolds in low spinning samples.[14]

Dipolar interactions have been extensively applied for investigating the geometric and electronic structure of the solid state. Since the internuclear dipolar coupling, D, scales with the gyromagnetic ratios (γ) of the two spins I and S and the inverse third power of the distance r_{IS}, according to the equation:

$$D = \frac{\mu_0}{4\pi} \frac{\hbar \gamma_I \gamma_S}{r_{IS}^3}$$

longer distance information can be preferentially obtained with high-γ nuclear spins such as ^{1}H and ^{19}F.

In high resolution spectra dipolar coupling are normally averaged out under MAS conditions owing to its dependence to the geometric factor ($3\cos^2\theta$-1); however, coupling information are of paramount importance to measure internuclear distances or to establish connectivities for structure elucidation. Although averaged by MAS, it can be reintroduced in the spectra by applying during the evolution period a series of RF pulses.[15] Rotational-echo double resonance (REDOR) technique reported by Schaefer and Gullion,[16] consists of two π pulses applied on spin S per rotor period, which prevents the refocalization of the I-S dipolar coupling at the end of each full rotation. The difference between the intensity of I recorded with this pulse sequence and that obtained in a reference experiment where no pulses are applied to spin S, is reported as a function of rotation period. The elegant technique allows to accurately determine the internuclear distances between atoms like ^{13}C-^{15}N (up to about 5 Å), ^{13}C-^{31}P (up to about 6 Å) and ^{13}C-^{19}F (up to about 8 Å) and has been applied, for example, for the distance evaluation in isotopically enriched ^{13}C-^{15}N pairs of amino acid and peptide fragments.[17] Further developments of recoupling sequences are Dipolar Recovery at the Magic Angle (DRAMA),[18] a rather simple pulse sequence of strong 90° pulses introduced by the Ticko's group, Transferred Echo Double Resonance (TEDOR),[19] the radio-frequency driven recoupling (RFDR) suggested by Griffin and co-workers, which is based on strong 180° pulses,[20] and symmetry-based sequences introduced by M. Lewitt and coworkers.[21]

Transfer of Population in Double Resonance (TRAPDOR)[22] and 'Rotational-Echo, Adiabatic Passage, Double Resonance' (REAPDOR)[23] have been proposed for evaluating dipolar couplings between spin-1/2 and quadrupolar nuclei. Back-to-back (BABA) sequence has been used in cases where spin pairs are strongly dipolarly coupled.[24] BABA is also used in heteronuclear correlation, where the double-quantum coherence between two different spins is created by applying a pulse sequence on both spin channels simultaneously.

All these techniques, which require neither isotopic labeling nor crystalline materials, have been extensively used to investigate packing and weak interactions on the building blocks of supramolecular systems. Then if one-dimensional spectra give chemical information via the chemical shift, ^{1}H-X FSLG-HETCOR and ^{1}H DQ MAS experiments enable a qualitative and quantitative determination of the internuclear distance in rigid systems. Indeed, the ^{1}H-^{13}C "on-resonance" CP HETCOR provides unambiguous ^{1}H signal assignments through the correlations with sharper ^{13}C peaks. In this sequence the polarization transfer occurs during a very short time, namely the contact time (CT). For longer CT, the detection of additional ^{1}H-^{13}C coherences provides further geometrical constraints if analyzed with respect to the formation of ^{1}H-^{1}H polarization coherences. For a complete analysis, the use of an "off-resonance" CP achieved by a Lee-Goldburg spin-lock (LG-CP) efficiently suppresses unwanted ^{1}H-^{1}H spin exchange leading to the observation of long-range ^{1}H-^{13}C contacts only up to 3.0-3.3 Å.[25]

Rotor synchronized two dimensional ^{1}H DQ MAS experiment acquired at fast MAS (>30 kHz) avoids the presence of spinning sideband patterns and results in improving the sensitivity and reducing the experimental time. With this technique neighboring hydrogen atoms are able to generate DQ coherence (DQC). Thus, specific information about intra- and intermolecular proton-proton spatial proximities[26] becomes available. In DQ MAS spectra a DQC between two like protons gives rise to a diagonal peak at the positions (ω_A, $2\omega_A$), whereas a DQC between two unlike protons A and B gives rise to two crosspeaks arranged symmetrically either side of the diagonal at frequencies (ω_A, $\omega_A+\omega_B$) and (ω_B, $\omega_A+\omega_B$).

The combination of physical rotation of the sample under MAS with the application of carefully synchronized RF pulses (PMLG[27] or DUMBO[28]) in CRAMPS sequences produces considerable line-narrowing in the ^{1}H solid state spectra compared to the use of fast

MAS alone. The resolution improvement of the elegant CRAMPS techniques with compare to the brutal force of MAS has been thoroughly reviewed by S. P. Brown.[29] ^{1}H–^{1}H DQ-SQ CRAMPS[30] and ^{1}H (DQ DUMBO)–^{13}C (SQ) refocused INEPT[31] spectra significantly enhance the resolution of DQ correlation peaks. The combining use of such pulse sequences with first-principles GIPAW (gauge-including projector augmented wave) NMR chemical shift calculations have been extensively employed to provide complete assignment of solid-state resonances.[32] ^{1}H (DQ)-^{13}C correlation spectra correlates a high-resolution ^{1}H DQ dimension with a ^{13}C single quantum (SQ) dimension using the refocused INEPT pulse-sequence element to transfer magnetization *via* one-bond ^{13}C-^{1}H *J* couplings. In this way the separation of the ^{1}H DQ coherences by means of the resolved ^{13}C resonances allows a ^{1}H DQ coherence due to two ^{1}H nuclei that are directly bonded to two distinct (directly bonded) carbon atoms to be identified. Thus, this spectrum allows, in principle, the carbon skeleton of a molecule to be mapped out in an analogous fashion to the case of ^{13}C-^{13}C correlation spectra (refocused INADEQUATE[33] or DQ-filtered COSY[34] experiments). In this case, however, it takes advantage of the higher probability of having adjacent a ^{1}H-^{13}C pair (1 in 100) instead of two adjacent ^{13}C nuclei (1 in 10000). In many polymorphs or co-crystals the investigation of the three-dimensional packing arrangements requires the study of proximities between nitrogen and proton nuclei that are particularly useful for the location of hydrogen bonds.[35] Such ^{14}N-^{1}H proximities can be readily probed using novel 2D ^{14}N-^{1}H HMQC experiment where indirect detection of the ^{14}N lineshapes are observed via proton acquisition.

The experimental boundaries of NMR spectroscopy have been greatly extended not only by the searching of new pulse sequences, but also by the continuous development of stronger magnets, more sensitive probes, operating at higher MAS rates, and improved computational tools. The combination of such efforts has led to dramatic progress for the NMR crystallography discipline. In the next paragraphs recent examples of application of the use of dipolar interaction for the structural analysis of polymorphs and cocrystals are reported.

Dipolar Interaction in Polymorphs

The polymorphism occurrence is the existence of more than one crystal structure for a given compound. Approximately 30% of organic compounds are believed to exhibit polymorphic forms.[36] Polymorphism represents a challenging phenomenon in many areas of research and industry such as pigments and dyes, explosives, agrochemicals and pharmaceuticals, where careful control over production is necessary to ensure that polymorphic or pseudopolymorphic transformations do not occur.[37] A deeper knowledge of properties, stabilities and structures of polymorphs is, for example, one of the most important goals for pharmaceutical industries,[38] since solid-state properties of drugs significantly influence the bioavailability and stability of the final product. Investigation of the most suitable form in a series represents a key step in the choice of a drug in order to avoid problems associated with late-phase changes or manufacturing conversions. Thermodynamic and kinetic data are essential parameters that are usually obtained by a series of methods able to determine solubility and intrinsic dissolution, melting behavior, metastable zone widths and occurrence domains.

A thorough study of the behavior of a polymorph starts from its structural analysis. Indeed, crystal packing, conformation and hydrogen bonding arrangements are fundamental in determining the final solid-state properties of a given form. Particle size and crystallinity are also closely related.

In this contest, SSNMR plays a fundamental role in assisting, complementing and supporting both X-ray single crystal and powder diffraction.

For instance, SSNMR is a potentially powerful tool for the investigation of the protonation states of molecules via ^{1}H, ^{13}C, and ^{15}N chemical shifts.[39,40,41] In the case of weak interactions SSNMR techniques provide the best contribution to diffraction techniques due to the marked sensitivity of NMR parameters of the nuclei (in particular hydrogen, carbon, and nitrogen) directly involved in chemical bonding. Determination of internuclear distances by SSNMR techniques plays a key role in the structure characterization and conformational analysis in polymorphs. It has been demonstrated that ^{15}N-^{13}C REDOR NMR spectroscopy is a very sensitive technique for studying conformational studies of organic solids. A paradigmatic case[42] is the ^{15}N (labeled)-^{13}C (natural abundance) REDOR experiment applied to three modifications of ^{15}N-octyl-D-gluconamide, namely GA I, GA II and GA III (Scheme 1 and Fig. 1). The structure of GA I has been determined by X-ray spectroscopy, whereas it was not possible to obtain single crystals suitable for GA II and GA III due to their poorly crystallizing behavior. REDOR experiment applied on ^{15}N labelled samples allowed the measurement of several dipolar couplings in a single experiment. The experimental values for the ^{13}C-^{15}N dipolar couplings are in the range of 40 to 1.2 kHz and have been converted into distances of 1.4 to 4.07 Å. Then the data obtained by NMR allowed the determination of internuclear distances and have been used also for an unambiguous assignment of the ^{13}C chemical shifts.

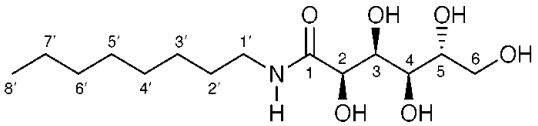

Scheme 1 ^{15}N-octyl-D-gluconamide

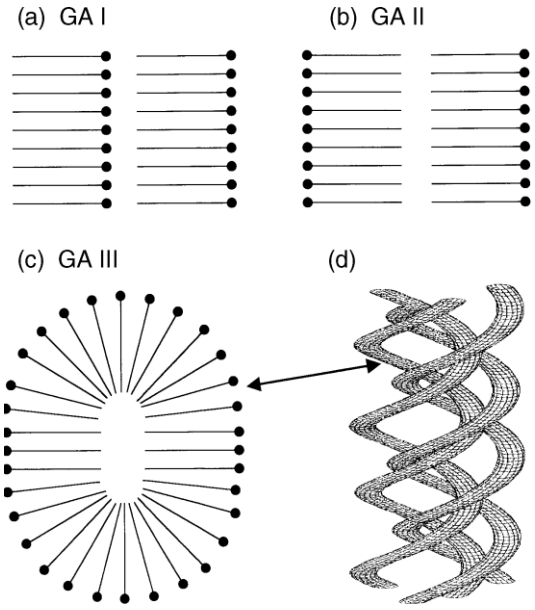

Fig. 1 Schematic superstructures of N-octyl-D-gluconamide in its different modifications, sugar head groups are represented by black discs and the alkyl chains by lines. (a) Simple monolayer crystal with linear head-to-tail arrangement of the molecules (GA I). (b) Bilayer crystallites with head-to-head arranged molecule pairs (GA II). (c) Micellar Fiber modification (GA III) showing a tail-to-tail arrangement of 24 gluconamide molecules, which gives long fiber structures intertwining to the extended quadruple helix (d). X-ray structure of GA I.

The reliability of the method has been proved for GA I, where the X-ray structure is available: the distances found by REDOR experiment were in very good agreement with the crystallographic parameters.
In the case of GA II and GA III the range of distances measured allowed the accurate determination of possible sets of torsion angles, which describe the conformations of the molecules in the vicinity of the ^{15}N label (Scheme 2 and Fig. 2).

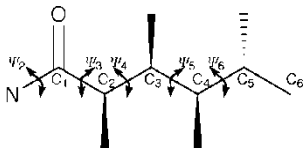

Scheme 2 Definition of the torsion angles Ψ_2, Ψ_3, Ψ_4, Ψ_5, Ψ_6 which determine the conformations of the head groups.

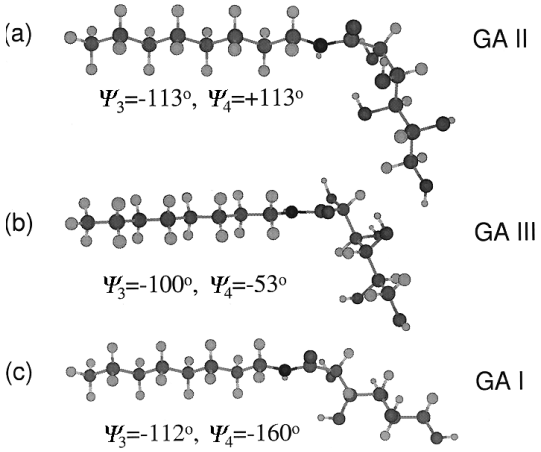

Fig. 2 Steric view of the conformations of GA; (a) GA II; $\Psi_3 = 113°$, $\Psi_4 = 113°$; (b) GA III; $\Psi_3 = 100°$, $\Psi_4 = 53°$; (c) GA I; $\Psi_3 = 112°$, $\Psi_4 = 160°$.

SSNMR studies are often devoted to the comprehension of the hydrogen bonding network in a number of intriguing hydrogen-bonded polymorph molecules. The final aim of such studies is mainly the interpretation of the role of intermolecular bonding in the process of molecular recognition that leads to crystallization of organic molecules.
^1H DQ spectroscopy represents a powerful method for identifying proton-proton intra- or intermolecular proximities up to ~3.5 Å. By employing advanced techniques in homonuclear ^1H decoupling that deliver high-resolution ^1H spectra, such as ^1H DQ CRAMPS,[43] relevant information on hydrogen bond network can be extracted that are not usually available with other experiments.[44]

An intriguing example of SSNMR application to the detection of hydrogen bond interactions is offered by the study of 2-thiobarbituric acid polymorphs.[45] With a total of six crystal forms and one hydrated form, 2-thiobarbituric acid represents the richest collection of examples of tautomeric (keto or enol form, see Scheme 3) polymorphism so far reported in the literature for a single molecule.

Scheme 3 The keto (a) and enol (b) tautomers of 2-thiobarbituric acid with the atomic numbering used.

By combining single-crystal X-ray diffraction, 1D and 2D (^{1}H, ^{13}C, and ^{15}N) SSNMR spectroscopy, Raman spectroscopy and X-ray powder diffraction at variable temperature it was possible to establish that the 2-thiobarbituric molecules are present in the enol form in the crystalline form II and in the hydrate form, whereas only the keto isomer is present in crystalline forms I, III, V and VI. A 50:50 ordered mixture of enol/keto molecules is present in form IV. However the role of hydrogen bond interactions in determining the relative stability of the polymorphs and as a driving force in the conversions has been ascertained only through ^{1}H DQ MAS and ^{1}H-^{13}C FSLG LG-CP HETCOR experiments.
The hydrogen-bond region of the ^{1}H-^{13}C FSLG LG-CP HETCOR and the ^{1}H DQ MAS spectra of form IV are reported in Fig. 3 and 4 together with a schematic representation of the heteronuclear and homonuclear proximities between keto and enol molecules.

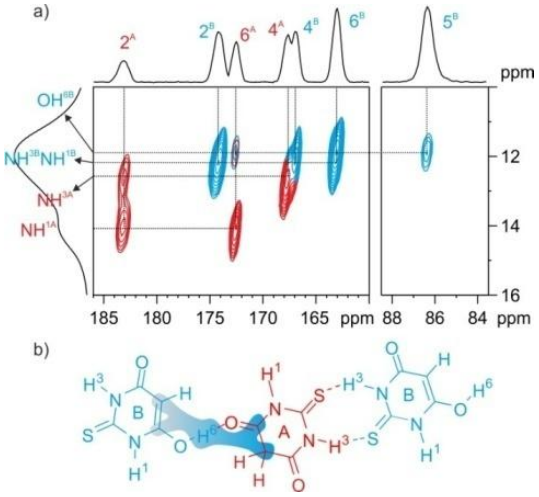

Fig. 3 a) ^{1}H–^{13}C FSLG LG-CP HETCOR spectrum (hydrogen-bond region) of form IV of 2-tiobarbituric acid acquired with a contact time of 2000 ms. Label "A" and "B" refer to keto and enol tautomers, respectively. b) Schematic representation of the ^{1}H-^{13}C intermolecular proximities. (Reproduced with permission from John Wiley and Sons)

The presence of eight signals in the ^{13}C spectrum of form IV (peak at δ = 42.6 not shown in fig. 3) reveals the existence of two molecules in the unit cell, whereas the CH (δ= 86.4 ppm) and CH_2 (δ= 42.6 ppm) resonances indicate the presence of both A and B isomers in the unit cell (Fig. 5).
Careful inspection of the ^{1}H-^{13}C FSLG LG-CP HETCOR spectrum allows the identification of all ^{1}H-^{13}C intra- and intermolecular correlations as, for example, the proximities of the OH proton $H6_B$ at δ =11.9 ppm with $C6_B$ (δ =167.1 ppm), $C6_A$ (δ =172.6 ppm) and $C5_B$ (δ =86.4 ppm) carbon atoms in agreement with the X-ray data. The presence of five hydrogen bonds in Form IV, the thermodynamically most stable form at room temperature, involving one O-H···O, two N-H···O and two N-H···S interactions on each molecule in the asymmetric unit cell, was revealed by the ^{1}H DQ MAS spectrum (Fig. 4). Intramolecular and intermolecular proximities were clearly highlighted in such spectrum.

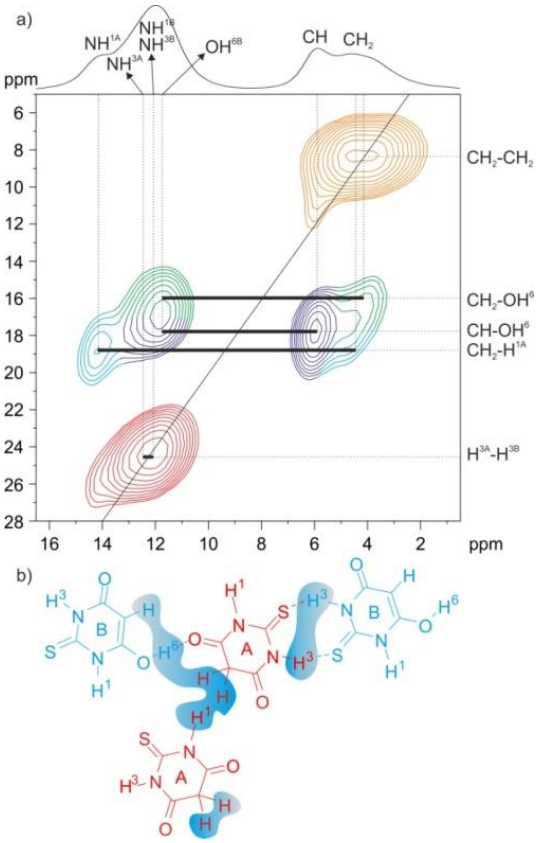

Fig. 4 a) ^{1}H DQ MAS spectrum of form IV of 2-thiobarbituric acid acquired at a spinning speed of 32 kHz. b) Schematic representation of the intra- and intermolecular ^{1}H-^{1}H proximities. (Reproduced with permission from John Wiley and Sons)

All these information combined with the strength of intermolecular interaction obtained by the proton chemical shifts opened the possibility of a deeper knowledge of the relative stability in the family of 2-thiobarbituric polymorphs. This depends on a complex balance of the tautomeric character of the molecule in the keto or enol forms and the strength of intermolecular interactions.
It is worth noting that SSNMR methods provide also direct evidence of the degree of conversion between the keto–enol forms by mechanochemical reactions in samples where the longer distance order have been lost. An example is represented by the barbituric acid.

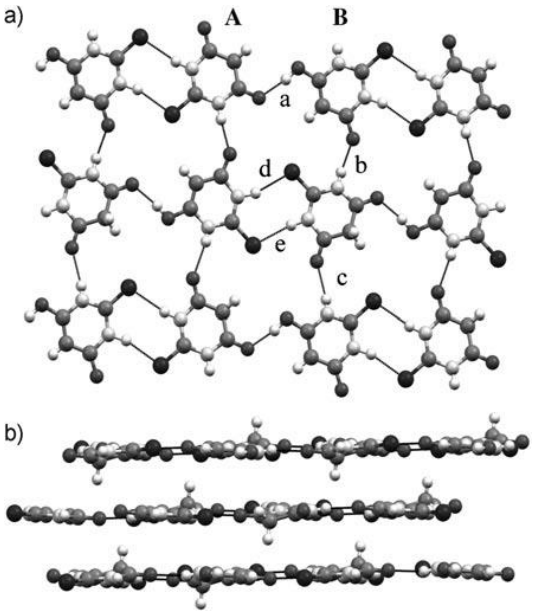

Fig. 5 Form IV of 2-thiobarbituric acid: a) hydrogen-bond pattern between the keto (A) and enol (B) isomers within the 2D-layer; b) stacking of the layers. (Reproduced with permission from John Wiley and Sons)

This molecule is known in different polymorphs: the keto tautomeric form I[46] (tautomer **1** in Scheme 4) that is the most stable form in the gas phase, the commercial phase II,[47] a high temperature phase III[48] and the recently discovered tautomeric polymorph IV that

resulted to be the thermodynamically most stable polymorph at room temperature.[49] All attempts to recrystallize form IV as a single crystal failed, whereas the grinding or milling processes resulted in powders of low crystallinity.

However it was possible to obtain the structure of polymorph IV that consists of molecules in the enol form (tautomer **2** in Scheme 4) by means of simulated annealing from X-ray powder data. Subsequently, the structure was refined by the Rietveld method using synchrotron and neutron data. Dipolar connectivity and chemical shift information obtained from SSNMR experiments provided in this case qualitative knowledge that assisted in obtaining the best possible powder structure solution from the X-ray data.

Analysis of ^{15}N LG-CP build-up curves on an ^{15}N natural-abundance sample of polymorph IV (Fig. 6), afforded N-H distances of 1.04±0.02 Å for both ^{15}N signals (δ=110.7 and 122.6 ppm). The ^{1}H-^{15}N heteronuclear distances were accurately extracted from Lee-Goldburg cross polarization (LG-CP) build-up curves, recorded at high MAS rates (12 kHz) (Fig. 6A). The efficient suppression of unwanted ^{1}H homonuclear dipolar interactions during CP achieved by LG spin-lock leads to oscillatory behaviour of ^{15}N magnetization reflecting the strength of the ^{1}H-^{15}N heteronuclear dipolar coupling only. This time evolution could be evaluated with respect to the interatomic distance through the heteronuclear dipolar coupling constant. The Fourier transform of the time-oscillatory ^{15}N magnetization LG-CP build-up curves provides dipolar broadened response profiles similar to Pake doublets (Fig. 6B) whose peak-to-peak distance is $\delta_0=\Delta\omega/2\pi=\omega_d\cos\theta_m$.

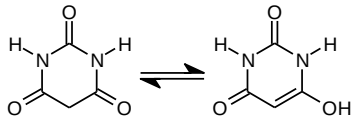

1 **2**

Scheme 4 Keto (1) and enol (2) tautomers of barbituric acid.

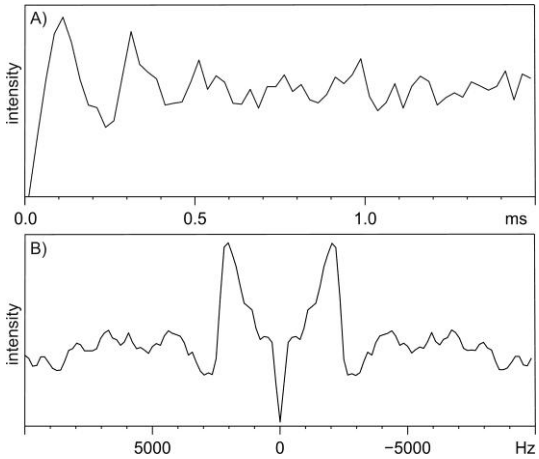

Fig. 6 LG-CP build-up curve (A) and its Fourier transform (B) for the NH group resonating at 110.7 ppm, extracted from the 2D experiment. (Reproduced with permission from John Wiley and Sons)

These SSNMR data are in agreement with the enol structure 2 revealed by neutron powder data. This crystal structure is in agreement with ^{1}H-^{1}H and ^{1}H-^{13}C proximities obtained from ^{1}H DQ MAS and ^{1}H-^{13}C FSLG LG-CP HETCOR SSNMR experiments. These techniques also allowed the complete ^{1}H and ^{13}C peak assignment, which attributes the short resonance-assisted O-H···O hydrogen bond to the ^{1}H signal at δ =15.0 ppm thus to a strong interaction.[50]

The higher stability of the enol form in the solid state is explained by the formation of an additional strong hydrogen bond in the crystal, leading to a more favorable lattice energy.

NMR crystallography approach is particularly useful not only in cases where single crystals are not available but also when structure solution from powder data is not possible (or accessible). This is the case, for example of didanosine (2',3'-dideoxyinosine), a reverse transcriptase inhibitor effective against HIV. In order to address polymorphism issues on the commercial form of didanosine and a sample recrystallized from a dimethylsulfoxide solution using supercritical CO_2 as an antisolvent,[51] 2D ^{1}H DQ CRAMPS (Combined Rotation And Multiple Pulse Spectroscopy) and ^{1}H-^{13}C FSLG on- and off-resonance CP HETCOR experiments have been performed. Information about ^{1}H-^{1}H and ^{1}H-^{13}C intra- and intermolecular proximities obtained by means of the 2D NMR experiments combined with the X-ray powder allowed to conclude that commercial and supercritical antisolvent re-crystallized didanosine possess very similar hydrogen bond network and molecular conformation, but different packing. It is worth noting that NMR data could suggest the presence of enol form on both commercial and re-crystallized didanosine samples.

A nice example of combination of advanced high-resolution ^{1}H SSNMR experiments with first-principles GIPAW chemical shift calculations and multispin density-matrix simulations is represented by the paper published by S.P. Brown and coworkers on the γ polymer of indomethacin (Scheme 5), a nonsteroidal drug used as anti-inflammatory, antipyretic and analgesic.[52]

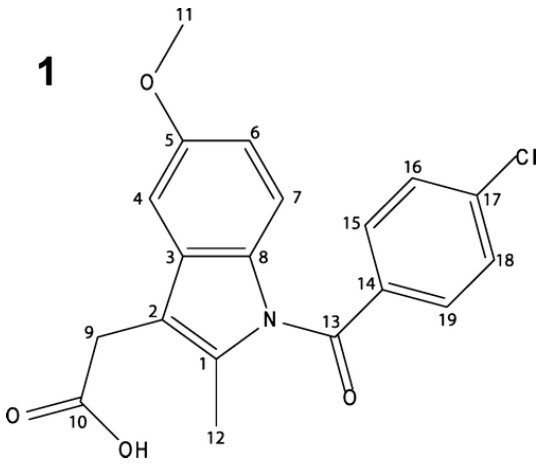

Scheme 5 The indomethacin molecule.

Crystal structures have been solved only the α and γ forms.[53] Proton-proton proximities in the solid state for H_{aliph}-H_{aliph}, H_{aliph}-H_{arom}, H_{arom}-H_{arom} were detected by ^{1}H DQ CRAMPS of γ-indomethacin recorded at 600 MHz (Fig. 7). Other proximities were found for the OH proton to another OH proton (δ_{DQ} = 25.4 ppm) and to aromatic CH protons (δ_{DQ} =19.9 ppm). Particularly useful for the characterization was the ^{1}H single-quantum (SQ) (DUMBO)-^{13}C SQ refocused INEPT[31] experiment that with a short $\tau=\tau'$=1.12 ms spin echo duration ensured that all the peaks are related to C-H single bond correlations. These data are combined with GIPAW chemical shift calculation for the full periodic crystal structure for the complete assignment of the NMR resonances.
Furthermore, the ^{1}H DQ integrated experimental intensity builds up (blue dashed lines) was analyzed as a function of the total DQ recoupling time, τ_{rcpl}, for the last two DQ peaks at the OH single-quantum (SQ) resonance (δ_{DQ} = 25.4 and 19.9 ppm reported at Fig 8a and 8b, respectively).

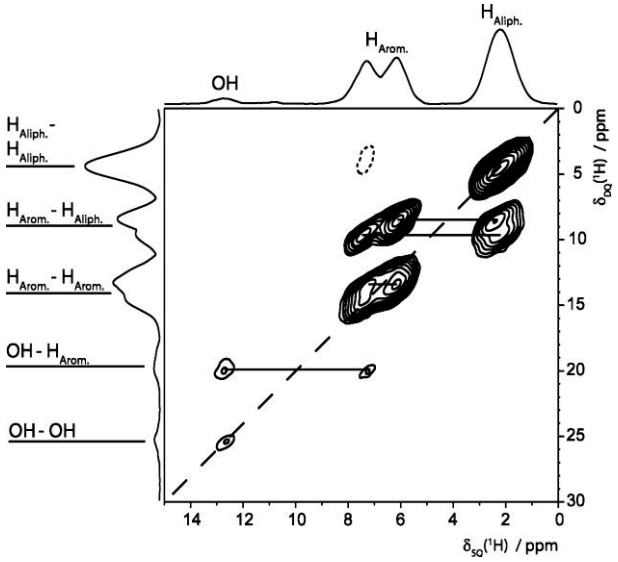

Fig. 7 ^{1}H DQ CRAMPS spectrum of γ-indomethacine with skyline projections. (Reproduced with permission from American Chemical Society)

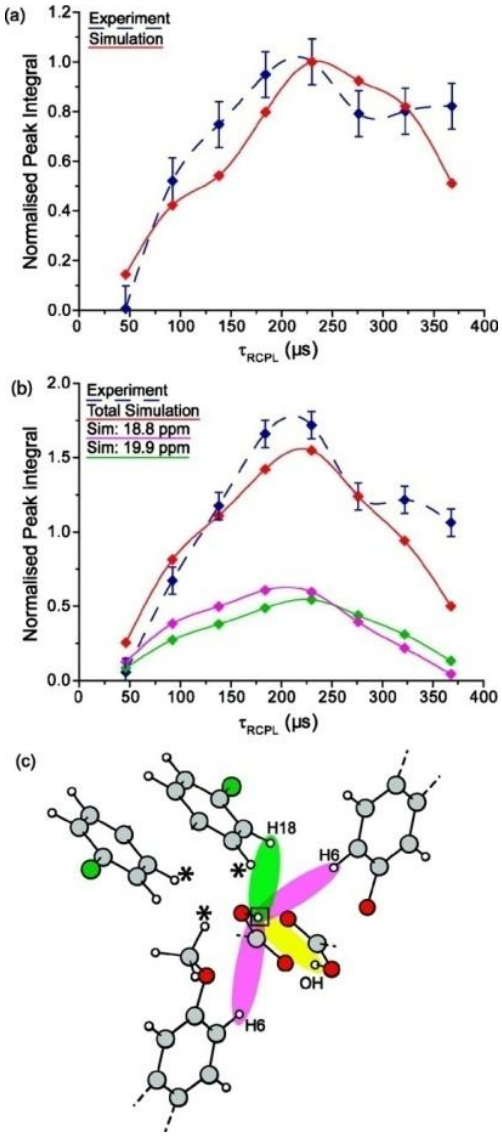

Fig. 8 (a, b) ^{1}H DQ build-up curves as a function of the total DQ recoupling time, τ_{rcpl}, for the (a) OH-OH DQ peak at δ_{DQ} = 25.4 ppm and (b) the OH-CH aromatic DQ peak at δ_{DQ} = 19.9 ppm. Blue dashed lines are refereed to integrated experimental intensities extracted from ^{1}H DQ CRAMPS spectra. In a, the red solid line corresponds to the simulated peak intensity (SPINEVOLUTION58) for the single OH-OH proximity for the simulated cluster of eight spins (highlighted in yellow in c). In b the red solid line corresponds to the summed intensity for separate simulated ^{1}H DQCs resulting from proximities between the OH proton and 5 different aromatic protons: H18, 2 x H6, H15 and H19. Green and pink solid lines are related to the separate simulated intensities for the OH-H18 (δ_{DQ} = 19.9 ppm, 2.48 Å) and OH-H6 (δ_{DQ} = 18.8 ppm, 2.89 and 3.18 Å) DQ peaks respectively. (Reproduced with permission from American Chemical Society)

The experimental values were compared with the simulated data (SPINEVOLUTION58) of the eight-spin density-matrix for a cluster of ^{1}H nuclei corresponding to the OH proton and the seven nearest protons for the (a) OH-OH DQ peak (δ_{DQ} = 25.4 ppm) and (b) the OH-CH aromatic DQ peak (δ_{DQ} = 19.9 ppm). Separate contributions from the OH-H18 and OH-H6 proton pairs are also reported in Fig. 8.

According to the assumption proposed by Bradley *et al.*[54] that the relative intensity of DQ peaks due to separate pairs of ^{1}H nuclei is given, to a good approximation, by the ratio of the squares of the corresponding dipolar coupling constants, and hence to the inverse ratio of the H-H distances to the sixth power, the authors were able to demonstrate that the intensity of the OH-CH aromatic DQ peak relative to that of the OH-OH DQ peak can be estimated equal to 1.52 in excellent agreement to both the summed simulated (red line) and experimental (dashed blue line) intensity in Fig. 8. Therefore, for the resolved OH resonances in the ^{1}H DQ CRAMPS spectrum of γ-indomethacin, the build-up of ^{1}H DQ intensity is a rich source of quantitative information about intermolecular H-H proximities. Finally much better resolution of the DQ peaks for the CH aromatic ^{1}H nuclei has been obtained by using the ^{1}H(DQ-DUMBO)-^{13}C(SQ) refocused INEPT[32] pulse sequence taking advantage of the much better resolution in a ^{13}C as compared to a ^{1}H spectrum.

Dipolar Interaction in co-crystals and salts

Co-crystalline materials are molecular materials constituted of two or more different molecules held together by supramolecular interactions.

Their formation represents an alternative and effective approach with respect to the polymorphism phenomenon for modulating chemical and physical behavior of a molecule. Indeed, the properties of the solid can be substantially changed by an adequate choice of the co-former, which would require the optimization of an entirely new set of intermolecular interactions, from strong and weak hydrogen bond interactions,[55] to halogen bonds[56] and London dispersion forces. This leads to new chemical formulations associated to new crystal packings, hence to new properties (thermal stability, solubility, dissolution rate, color, processability etc.). Usually co-formers are organic molecules chosen on the basis of their ability to form supramolecular aggregates with the main component but also inorganic salt have been used more frequently in the last years.[57]

As for the polymorphism, the SSNMR is a growing fundamental tool for the characterization of co-crystalline phases. Indeed, under the impetus of the sustainable chemistry, the number of solvent-free reactions leading to microcrystalline product not suitable for XRSCD analysis is increasing quickly in literature. Thus an appropriate use of the dipolar interaction can be essential for both helping XRPD indexing processes and providing evidence of co-crystal formation and elucidating hydrogen bond network. Furthermore, when X-ray diffraction gives an ambiguous answer, it allows understanding of whether the multicomponent crystal is a co-crystal or a molecular salt. Indeed, by helping the chemical shift assignment the analysis of the dipolar interaction can provide insights concerning the position of hydrogen atoms along hydrogen bonding axes.

This is the case of nine tenoxicam co-crystals achieved using solvent-drop grinding techniques.[58] 2D SSNMR methods were used to confirm co-crystal formation and determine structural aspects for co-crystals formed with saccharin, salicylic acid, succinic acid, and glycolic acid in comparison to form I and III of tenoxicam. Molecular association was demonstrated using both short- and long-range ^{1}H-^{13}C FSLG CP HETCOR. While short-range ^{1}H-^{13}C FSLG CP HETCOR (Fig. 9a), run with a contact time of 500 μs, provided a reliable and precise assignment of the ^{1}H resonances, a longer contact time (2 ms) (Fig. 9b) allowed for increased ^{1}H-^{1}H spin diffusion during the ^{1}H spin lock period prior to the CP transfer. The presence of spin-diffusion driven correlations between the glycolic methylenic carbon and tenoxicam aromatic protons showed direct evidence of intermolecular interactions between tenoxicam and glycolic acid.

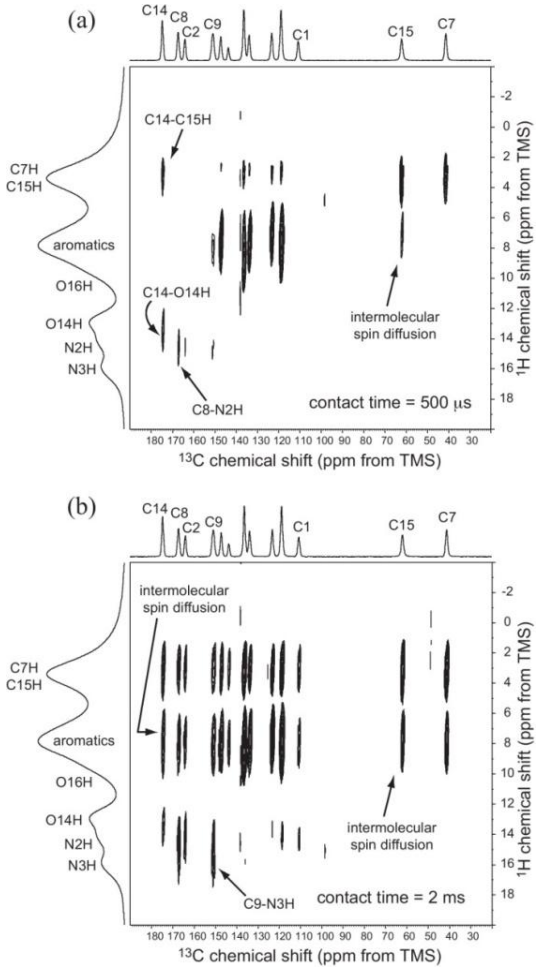

Fig. 9 2D ^{1}H-^{13}C FSLG CP HETCOR spectra of tenoxicam-glycolic acid co-crystal at contact time of 500 μs (a) and 2 ms (b) recorded with a spinning speed of 12.5 kHz. (Reproduced with permission from Elsevier)

In the same time, a strong correlation, observed in the ^{1}H DQ MAS, between tenoxicam N-H and glycolic carboxylic proton indicated that the two sites are in close proximity, suggesting a possible hydrogen bond arrangement between the molecular entities as reported in Scheme 6.

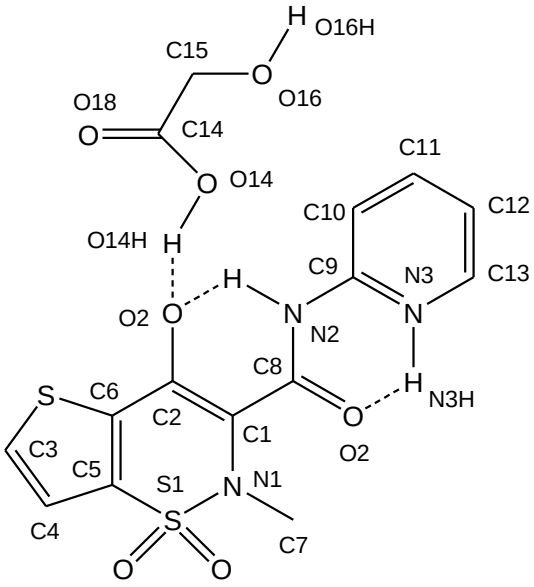

Scheme 6 Proposed hydrogen bond arrangement in tenoxicam-glycolic acid co-crystal.

A similar analysis performed by combining ^{1}H-^{13}C FSLG CP HETCOR and ^{1}H DQ MAS spectra allowed for the hydrogen bonding motif to be drawn in the nicotinamide-palmitic acid co-crystal.[59] Indeed, the ^{1}H-^{1}H (from ^{1}H DQ MAS) and ^{1}H-^{13}C (from FSLG CP HETCOR) proximities between palmitic carboxylic and nicotinamide aromatic moieties indicated the formation of a COOH···N(Ar) interaction.

The off-resonance variation of the HETCOR, the LG-CP HETCOR was successfully applied in assisting and simplifying the structure solution from X-ray powder data of lidocaine-succinate salt.[60] Indeed, long-range ^{1}H-^{13}C correlations (Fig. 10) allowed to confirm the presence of both acid chains linked via (acid)O-H···O(acid) hydrogen bond and (lido)N-H···O(acid) interaction between lidocaine and succinic acid. All proximities found by HETCOR and ^{1}H DQ CRAMPS agreed with the structure solved from XRPD. On the other hand, the analysis of the ^{13}C resonances around 160-179 ppm and of the ^{15}N signal around 14-29 ppm allowed ascertaining the transfer of a single proton from the acid to lidocaine with formation of one carboxylate and one ammonium group. Accordingly, the adduct could be described as molecular salt.

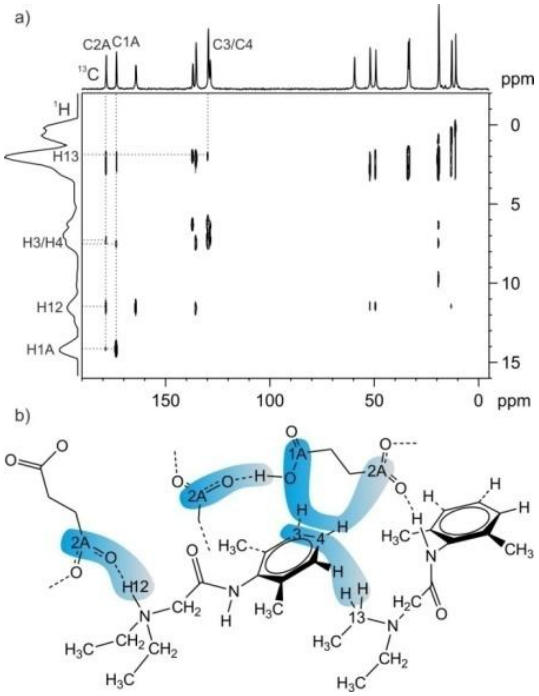

Fig. 10 (a) ^{1}H-^{13}C FSLG LG-CP HETCOR spectrum of lidocaine-succinate co-crystal recorded with a contact time of 2 ms and a spinning speed of 12 kHz. (b) Representation of the crystal packing of lidocaine-succinate co-crystal showing the main ^{1}H-^{13}C intermolecular proximities observed in the spectrum. (Reproduced with permission from American Chemical Society)

The most common application of the FSLG CP HETCOR is for the ^{1}H-^{13}C pair which has been used for the structure determination of many co-crystals, among them for instance also for naproxen-nicotinamide[61] and quinidine-methyl paraben.[62] In the first case, from the ^{1}H-^{13}C FSLG CP HETCOR NMR experiment (contact time of 5ms), two different supramolecular synthons, carboxylic

acid-amide and carboxylic acid-pyridine ring, were found between naproxen and nicotinamide (Scheme 7a and 7b). In both synthons the carboxylic group of the naproxen in the co-crystal was a nonionized form.
In the second case a series of correlations evidenced close spatial proximity of methyl paraben to quinidine providing insights on local conformation and hydrogen-bonding (Scheme 7c). These were also supported by DFT quantum-chemical computations. All evidences clearly ruled out a possible salt formation.

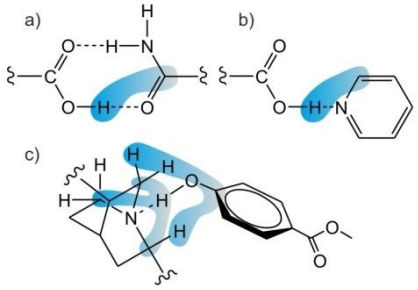

Scheme 7 Supramolecular synthons suggested by the ^{1}H-^{13}C proximities (highlighted in light blue) in naproxen-nicotinamide (a and b) and quinidine-methyl paraben (c) co-crystals.

However, the literature presents also the exploiting of more "exotic" pairs to be probed such as for instance ^{1}H-^{19}F, ^{19}F-^{13}C or ^{14}N-^{1}H.[59,63] These heteronuclear correlation experiments, however, often require the use of uncommon HFX triple resonance probes or high magnetic field (>800 MHz) at very fast MAS (>60 kHz).
The ^{1}H-^{19}F FSLG CP HETCOR, in its off-resonance version, was used to characterized the ternary complex of caffeine, succinic acid, and 1,4-difluorobenzene.[59] The inter- and intramolecular correlations observed in the spectrum (Fig. 11) between ^{19}F and aliphatic ^{1}H sites immediately verifies the presence of 1,4-difluorobenzene in the host framework. However due to the presence of aliphatic protons on both caffeine and succinic acid, the specific interaction could not be identified.

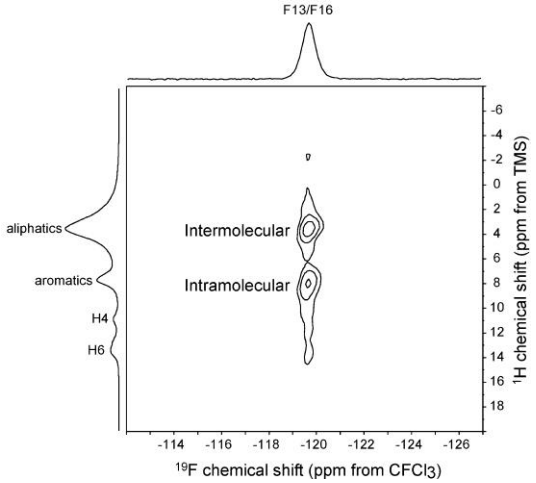

Fig. 11 ^{1}H-^{19}F LG-CP HETCOR of caffeine-succinic acid-1,4-difluorobenzene co-crystal. Spinning speed 14 kHz, contact time 200 μs. The ^{19}F CPMAS (ν_r =14 kHz) and ^{1}H MAS (ν_r =35 kHz) spectra are shown as projections. (Reproduced with permission from American Chemical Society)

On the other hand, the ^{19}F-^{13}C FSLG CP HETCOR was introduced to characterize a series of 5-fluorouracil and thymine solid solutions with variable composition (with $0.1<\chi<0.9$).[63] In particular, it was instrumental for determining the position of the fluorine atom in the asymmetric unit. This has been done by comparing F-C correlations observed in the ^{19}F-^{13}C FSLG CP HETCOR (contact time of 3 ms) and F···CH_3 proximities for two possible fluorine crystallographic positions.
Two-dimensional ^{14}N-^{1}H heteronuclear multiple-quantum correlation (HMQC) MAS NMR spectra were recorded for identifying the correct supramolecular arrangement in nicotinamide-palmitic[64] and acid indomethacin-nicotinamide co-crystals.[65] In the former example, the presence of a correlation peak in the ^{14}N-^{1}H HMQC spectrum between the nitrogen of nicotinamide and the carboxylic acid hydrogen in palmitic acid constituted unambiguous evidence for the formation of an intermolecular N···H-O hydrogen bond in the co-crystal. This is in agreement with the N1···H1 distance measured (1.7 Å) from the geometry optimized crystal structure which confirmed the neutral nature of the adduct.
In the latter example, by playing with the "mixing time", in this case the rotary resonance recoupling (R^3) duration (τ_{rcpl} = 130 μs or 670 μs), it has been possible to selectively analyze correlation peaks corresponding to one-bond or longer-range N···H connectivities (Fig. 12b and 12c). These allowed also the correct assignment of the two nicotinamide NH_2 ^{1}H chemical shifts at 7.3 and 9.0 ppm and of the ^{14}N resonances at about -40 and +140 ppm to the non-protonated nitrogen atoms of indomethacin and nicotinamide, respectively. Furthermore, ^{1}H-^{1}H proximities obtained from ^{1}H DQ MAS spectrum (Fig. 12a) agreed with these suggestions allowing to discard other possible supramolecular arrangements.

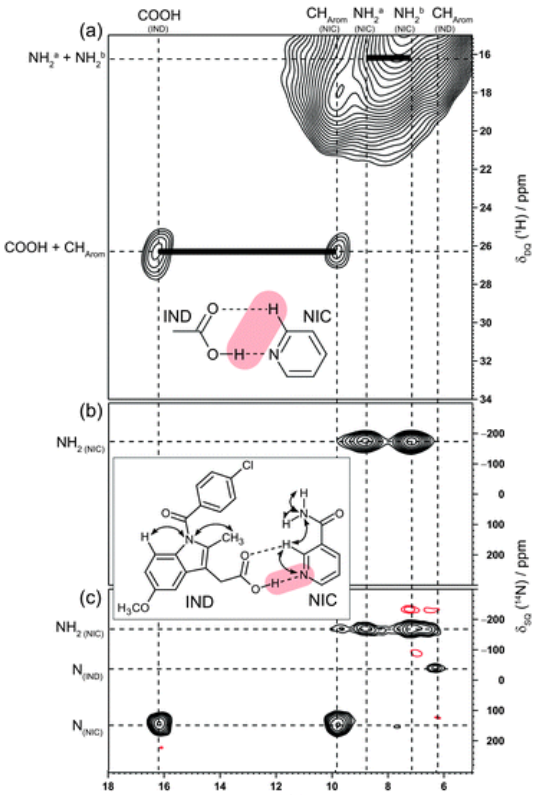

Fig 12 ^{1}H DQ MAS spectrum (a) and ^{14}N-^{1}H HMQC spectra with τ_{RCPL} = 130 μs (b) and τ_{rcpl} = 670 μs (c) of indomethacin-nicotinamide co-crystal. (Reproduced with permission from American Chemical Society)

This case was interesting also for the use of the ^{1}H-^{13}C refocused INEPT pulse sequence in its ^{1}H(SQ)-^{13}C(SQ) version instead of the more common FSLG HETCOR or MAS-J-HMQC[66] for confirming the ^{13}C assignment. While the ^{1}H(DQ)-^{13}C(SQ) correlation has been successfully applied for polymorph characterization (*see polymorph paragraph*), here the experiment was set of a short spin echo duration, $\tau = \tau' = 1.28$ ms, in order to ensure only one-bond CH correlations to be observed.

^{1}H DQ MAS has been widely used for achieving information on proton-proton proximities and thus on hydrogen bond networks in co-crystals. Some examples are co-crystals of 4,4'-bipyridine-pimelic acid (in three different polymorphic forms),[67] caffeine-succinic acid-1,4-dioxane, {4-(4-chloro-3-fluorophenyl)-2-[4-(methyloxy)phenyl]-1,3-thiazol-5-yl} acetic acid- nicotinamide,[59] quinidine-4-hydroxybenzoic acid,[68] tenoxicam-saccharin, tenoxicam-salicylic acid, tenoxicam-succinic acid.[58] The supramolecular synthons suggested together with the ^{1}H-^{1}H proximities are sketched in Scheme 8.

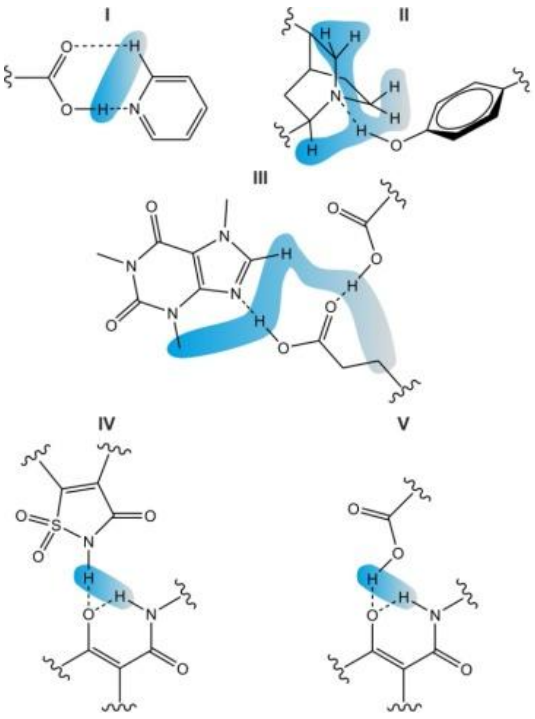

Scheme 8 Supramolecular hydrogen bonding arrangements as deducted from ^{1}H-^{1}H proximities (highlighted in light blue) for co-crystals (I) 4,4'-bipyridine-pimelic acid, (II) quinidine-4-hydroxybenzoic acid, (III) caffeine-succinic acid-1,4-dioxane (1,4-dioxane not drawn since not involved in hydrogen bonds), (IV) tenoxicam-saccharin, and (V) tenoxicam-salicylic acid and tenoxicam-succinic acid. For {4-(4-chloro-3-fluorophenyl)-2-[4-(methyloxy)phenyl]-1,3-thiazol-5-yl} acetic acid- nicotinamide adduct the ^{1}H-^{1}H proximities were not useful for suggesting hydrogen bonding interactions thus it is not reported.

On the other hand, its CRAMPS version, although providing much higher resolution, has been applied only for polymorph characterizations (*see polymorph paragraph*). This is probably due to the high degree of local order required by this experiment. This limits its applications when dealing with polycrystalline or structurally less-defined powdered samples that may result from mechanochemical reactions or early co-crystallization attempts. In such cases, the application of fast MAS is more convenient.
A rare example in the co-crystal word is the characterization of the already cited lidocaine-succinate co-crystal (*see above*).[60] Here, the improved resolution of the PMLG CRAMPS method[27] was compared to ^{1}H 1D MAS spectra. By means of a thorough analysis of the ^{1}H-^{1}H proximities observed in the ^{1}H DQ CRAMPS spectrum (Fig. 13) it has been possible to check the reliability of the molecular packing obtained from XRPD. In this case the comparison of the ^{1}H DQ CRAMPS spectrum with that of the lidocaine-fumarate co-crystal, whose structure was known from single crystal XRD analysis, was fundamental for the analysis of the ^{1}H-^{1}H proximities and thus for the packing determination.

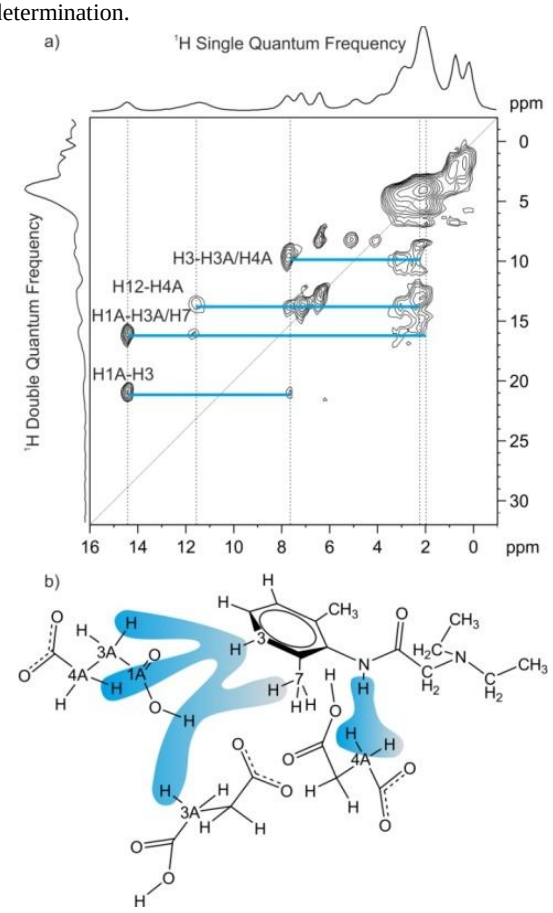

Fig. 13 a) 2D ^{1}H-^{1}H DQ CRAMPS of lidocaine-succinate co-crystal recorded with a spinning speed of 12.5 kHz. Solid blue orizontal bars indicate specific DQ coherences. b) Representation of the crystal structure showing the main ^{1}H-^{1}H intermolecular proximities characterizing crystal packing and HB enviroments. (Reproduced with permission from American Chemical Society)

Conclusions

In the last decades NMR crystallography has made a large and increasing contribution to the structure knowledge of crystalline and non crystalline solids. The possibility of determining by SSNMR techniques homo- and heteronuclear proximities also in disordered solids, makes them exceptionally powerful to solve crystallographic problems in the fascinating world of polymorphic and co-crystal forms. The resulting data have been used as restraints in the analysis of powder diffraction patterns to give full crystal structures. It is clear that these information are complementary not only to those obtained from diffraction studies but also from other spectroscopic techniques. The final result of such combination of techniques is a deeper knowledge of intermolecular interactions, hydrogen bonds and hydrogen location. Quantum mechanical computations of shielding are of paramount importance for the choice of the correct structure. It has been demonstrated that such approach can be applied to polymorphs, stoichiometric and non-stoichiometric solvates,

co-crystals, as well as to amorphous forms and to formulations.

Of course there are intrinsic drawbacks to the use of dipolar interaction for structural investigations. For instance, concerning rare nuclei an isotopic enrichment it is often required. On the other hand, in the case of abundance spins, there are still resolution limitations together with the theoretical difficulty of handle systems with more than 5-6 coupled spins.[69] However, we believe that the outgoing improvements of new SSNMR techniques able to evaluate dipolar interactions and internuclear distances will open a deeper knowledge of the intermolecular interactions and will stimulate further scientific efforts in the field of solid-state reactivity.

Notes and references

[a] *Department of Chemistry, University of Torino, Via Giuria 7, Torino, Italy. Fax: +39 011 6707855; Tel: +39 011 6707520; E-mail: roberto.gobetto@unito.it*

DOI: 10.1039/b000000x/

1 (a) Crystal Engineering: From Molecules and Crystals to Materials, Eds.: D. Braga, F. Grepioni, A. G. Orpen, Kluwer Academic Publishers, Dordrecht, 1999. (b) D. Braga, F. Grepioni, G. R. Desiraju, *Chem. Rev.*, 1998, **98**, 1375-1405. (c) M. D. Hollingsworth, *Science*, 2002, **295**, 2410-2413; (d) G. R. Desiraju, *Crystal Engineering: The Design of Organic Solids*, Elsevier, Amsterdam, 1989; (e) D. Braga, F. Grepioni, Coord. Chem. Rev., 1999, **183**, 19-41. (f) *The Crystal as a Supramolecular Entity. Perspectives in Supramolecular Chemistry, vol. 2*, Ed.: G. R. Desiraju, Wiley, Chichester, UK, 1996; (g) D. Braga, G. R. Desiraju, J. Miller, A. G. Orpen, S. Price, CrystEngComm, 2002, **4**, 500-509.

2 S.G. Patrick, *Cryst. Growth Des.*, 2007, **7**, 1007-1026.

3 (a) *Structure determination from powder diffraction data* (IUCR, Monographs on Crystallography No. 13; Eds. W. I. F. David, K. Shankland, L.M .McCusker, C. Baerlocher, Oxford University Press, New York, 2002. (b) *Crystal structure determination from powder diffraction data*; Ed. A. Clearfield, American Crystallographic Association, Buffalo, New York, 2002; Vol. 37.

4 (a) R. K. Harris *Analyst*, 2006, **131**, 351–373. (b) B. Elena, G, Pinatacuda, N. Misfud, L. Emsley, *J. Am. Chem. Soc.*, 2006, **128**, 9555–9560.

5 (a) Nonappa, M. Lahtinen, B. Behera, E Kolehmainen, U. Maitra, *Soft Matter*, 2010, **6**, 1748–1757; (b) V. Noponen, Nonappa, M. Lahtinen, A. Valkonen, H. Salo, E. Kolehmainen, E. Sievanen, *Soft Matter*, 2010, **6**, 3789–3796.

6 *NMR crystallography*, Eds. R. Harris,, R.E. Wasylishen, M.J. Duer, John Wiley & Sons Ltd. 2009.

7 R. K. Harris, Solid State Sciences, 2004, **6**, 1025-1037.

8 (a) M. Hunger, W. Wang, *Advances in Catalysis*, 2006, **50**, 149–225. (b) M. R. Chierotti, K. Gaglioti, R. Gobetto, M. Barbero, C. Nervi, *CrystEngComm*, 2012, **14**, 6732–6737.

9 (a) R. G. Griffin, *Nat. Struct. Biol.*, 1998, **5**, 508-512. (b) S. J. Opella, *Nat. Struct. Biol.*, 1997, **4**, 845-848. (c) W. T. Franks, A. H. Linden, B. Kunert, B.-J. van Rossum, H. Oschkinat, *Eur. J. Cell Biol.*, 2012, **91**, 340–348.

10 M. Geppi, G. Mollica, S. Borsacchi, C. A. Veracini, *Appl. Spectr. Rev.*, 2006, **43**, 202–302.

11 C. Bonhomme, C. Coelho, N. Baccile, C. Gervais, T. Y. Azaïs, F. Babonneau, *Acc. Chem. Res.*, 2007, **40**, 738–746.

12 (a) S. P. Brown, H. W. Spiess, *Chem. Rev.*, 2001, **101**, 4125–4155. (b) H. C. Hoffmann, M. Debowski, P. Müller, S. Paasch, I. Senkovska, S. Kaskel, E. Brunner, *Materials*, 2012, **5**, 2537-2572. (c) M. Geppi, S. Borsacchi, G. Mollica, C.A. Veracini, *Appl. Spectr. Rev.*, 2009, **44**, 1–89.

13 (a) J. K. Harper, D. M. Grant, Y. Zhang, P. L. Lee, R. VonDreele, *J. Am. Chem. Soc.*, 2006, **128**, 1547–1552. (b) D. A. Middleton, X. Peng, D. Saunders, K. Shankland, W. I. F. David, A. J. Markvardsen, *Chem. Commun*., 2002, 1976–1977.

14 (a) J. Herzfeld, A. E. Berger, *Chem. Phys.*, 1980, **73**, 6021-6030; (b) J. Viger-Gravel, I. Korobkov, D. L. Bryce, *Cryst. Growth Des.*, 2011, **11**, 4984-4995.

15 (a) G. De Paepe, J. R. Lewandowski and R. G. Griffin, *J. Chem. Phys.*, 2008, **128**, 124503. (b) B. Hu, J. Trebosc and J. P. Amoureux, *J. Magn. Reson.*, 2008, **192**, 112-122.

16 T. Gullion, and J. Schaefer, *J. Magn. Reson.*, 1989, **81**, 196-200.

17 (a) G. R. Marshall, D. D. Beusen, K. Kociolek, A. S. Redlinski, M. T. Leplaw, Y. Pan and J. Schaefer *J. Am. Chem. Soc.*, 1990, **112**, 963-966. (b) Y. Pan,; T. Gullion and J. Schaefer, *J. Magn. Reson.*, 1990, **90**, 330-340.

18 R. Tycko and G. Dabbagh, *Chem. Phys. Lett.*, 1990, **173**, 461-465.

19 A. W. Hing, S. Vega and J. Schaefer, *J. Magn. Reson., Ser A*, 1993, **103**, 151-162.

20 (a) A. E. Bennett, J. H. Ok, R. G. Griffin and S. Vega, *J. Chem. Phys.*, 1992, **96**, 8624-8627; (b) D. K. Sodickson, M. H. Levitt, S. Vega and R. G. Griffin, *J. Chem. Phys.*, 1993, **98**, 6742-6748.

21 M. H. Levitt, Encyclopedia of Nuclear Magnetic Resonance, Edited by D. M. Grant and R. K. Harris, John Wiley & Sons, Ltd, Chichester, 2002, **9**, 165-196.

22 C. P. Grey, W. S. Veeman and A. J. Vega, *J. Chem. Phys.*, 1993, **98**, 7711-7724.

23 E. Hughes, T. Gullion, A. Goldbourt, S. Vega and A. J. Vega, *J. Magn. Reson.*, 2002, **156**, 230-241.

24 (a) M. Feike, D. E. Demco, R. Graf, J. Gottwald, S. Hafner and H. W. Spiess, *J. Magn. Reson., Ser A*, 1996, **122**, 214-221; (b) W. Sommer, J. Gottwald, D. E. Demco and H. W. Spiess, *J. Magn. Reson., Ser A*, 1995, **113**, 131-134.

25 B. J.van Rossum, C. P. de Groot, V. Ladizhansky, S. Vega, H. J. M. de Groot, *J Am. Chem. Soc.*, 2000, **122**, 3465-3472.

26 (a) D. Braga, G. Palladino, M. Polito, K. Rubini, F. Grepioni, M. R. Chierotti, R. Gobetto, *Chem. Eur. J.*, 2008, **14**, 10149–10159. (b) I. Schnell, S. P. Brown, H. Y. Low, H. Ishida, H. W. Spiess, *J. Am. Chem. Soc.*, 1998, **120**, 11784–11795.

27 E. Vinogradov, P. K. Madhu and S. Vega, *Chem. Phys. Lett.*, 1999, **314**, 443-450.

[28] (a) D. Sakellariou, A. Lesage, P. Hodgkinson and L. Emsley, *Chem. Phys. Lett.*, 2000, **319**, 253-260. (b) A. Lesage, D. Sakellariou, S. Hediger, B. Elena, P. Charmont, S. Steuernagel and L. Emsley, *J. Magn. Reson.*, 2003, **163**, 105-113.
[29] S. P. Brown, *Prog. Nucl. Magn. Reson. Spectrosc.* 2007, **50**, 199−251.
[30] S. P. Brown, A. Lesage, B. Elena and L. Emsley, *J. Am. Chem. Soc.* 2004, **126**, 13230-13231.
[31] B. Elena, A. Lesage, S. Steuernagel, A. Bockmann and L. Emsley, *J. Am. Chem. Soc.*, 2005, **127**, 17296-17302.
[32] A. L. Webber, B. Elena, J. M. Griffin, J. R. Yates,T. N. Pham, F. Mauri, C.J. Pickard, A. M. Gil, R. Stein, A. Lesage, L. Emsley and S. P. Brown, *Phys. Chem. Chem. Phys.*, 2010, **12**, 6970–6983.
[33] A. Lesage, M. Bardet and L. Emsley, *J. Am. Chem. Soc.*, 1999, **121**, 10987-10993.
[34] (a) R. A. Olsen, J. Struppe, D. W. Elliott, R. J. Thomas and L. J. Mueller, *J. Am. Chem. Soc.*, 2003, **125**, 11784-11785; (b) L. L. Chen, R. A. Olsen, D. W. Elliott, J. M. Boettcher, D. H. H. Zhou, C. M. Rienstra and L. J. Mueller, *J. Am. Chem. Soc.*, 2006, **128**, 9992-9993; c) D. Lee, J. Struppe, D. W. Elliott, L. J. Mueller and J. J. Titman, *Phys. Chem. Chem. Phys.*, 2009, **11**, 3547-3553.
[35] S. Cavadini, *Progr. Nucl. Magn. Res. Spectr.*, 2010, **56**, 46-77.
[36] M. Kuhnertbrandstatter, M. Riedmann, *Mikrochim. Acta*, 1987, **2**, 107-120.
[37] J. Bernstein, *Polymorphism in Molecular Crystals*, Oxford University Press, Oxford, 2002, p. 352.
[38] H. G. Brittain, *Polymorphism in Pharmaceutical Solids*, Marcel Dekker, Inc, New York, 1999, p. 427.
[39] (a) Z. Gu and A. McDermott, *J. Am. Chem. Soc.*, 1995, **115**, 4282-4285 and references therein.
[40] D. Braga, L. Maini, G. de Sanctis, K. Rubini, F. Grepioni, M.R. Chierotti, R. Gobetto, *Chem.–Eur. J.*, 2003, **9**, 5538–5548.
[41] G.E. Hawkes, K.D.Sales, L.Y. Lian, R. Gobetto, *Proc. Royal Soc. London Series A-Math. Phys. and Eng.Sc.*, 1989, **424**, 93-111.
[42] I. Sack, S. Macholl, J. H. Fuhrhop and G. Buntkowsky, *Phys. Chem. Chem. Phys.*, 2000, **2**, 1781-1788.
[43] (a) I. Schnell, A. Lupulescu, S. Hafner, D. E. Demco, H. W. Spiess, *J. Magn. Reson.*, 1998, **133**, 61-69. (b) L. Mafra, R. Siegel, C. Fernandez, D. Schneider, F. Aussenac, J. Rocha, *J. Magn. Reson.*, 2009, **199**, 111-114.
[44] R. K. Harris, P. Hodgkinson, V. Zorin, J.-N. Dumez, B. Elena-Hermmann, L. Emsley, E. Salager, R. S. Stein, *Magn. Reson. Chem.*, 2010, **48**, S103-S112.
[45] M.R. Chierotti, L. Ferrero, N. Garino, R. Gobetto, L. Pellegrino, D. Braga, F. Grepioni, L. Maini, *Chem. Eur. J.* 2010, **16**, 4347–4358.
[46] W. Bolton, *Acta Crystallogr., Sect. B: Struct. Crystallogr. Cryst. Chem.*, 1963, **16**, 166–173.
[47] T. C. Lewis, D. A. Tocher and S. L. Price, *Cryst. Growth Des.*, 2004, **4**, 979–987.
[48] (a) D.M. Tobbens, J. Glinneman, M.R. Chierotti, J. van de Streek, D. Sheptyakov, *CrystEngComm* 2012, **14**, 3046-3055; (b) M. V. Roux, M. Temprado, R. Notario, C. Foce-Foces, V. N. Emel'yaneko and S. P. Verevkin, *J. Phys. Chem. A*, 2008, **112**, 7455–7465; (c) N. Zencirci, E. Gstrein, Ch. Langes and U. J. Griesser, *Thermochim. Acta*, 2009, **485**, 33–42.
[49] M. U. Schmidt, J. Brning, J. Glinnemann, M. W. Htzler, P. Mçrschel, S. N. Ivashevskaya, J. van de Streek, D. Braga, L. Maini, M. R. Chierotti, R. Gobetto, *Angew. Chem. Int. Ed.*, 2011, **50**, 7924–7926.
[50] M. R. Chierotti, R. Gobetto, Chem. Commun., 2008, 1621–1634
[51] R. Bettini, Menabeni, R. Tozzi, M. B. Pranzo, I. Pasquali, M. R. Chierotti, R. Gobetto, L. Pellegrino, *J. Pharm. Sci.*, 2010, **99**, 1855-1870.
[52] J. P. Bradley, S. P. Velaga, O. N. Antzutkin, and S.P. Brown, *Cryst. Growth Des.*, 2011, **11**, 3463–3471.
[53] (a) X. M. Chen, K. R. Morris, U. J.; Griesser, S. R. Byrn, J. G. Stowell, *J. Am. Chem. Soc.* 2002, **124**, 15012. (b) P. J. Cox, P. L. Manson, *Acta Crystallogr.* 2003, **E59**, 986.
[54] J. P. Bradley, C. Tripon,; C. Filip,; S. P. Brown, *Phys. Chem.Chem. Phys.*, 2009, **11**, 6941-6952.
[55] D. Braga, E. Dichiarante, G. Palladino, F. Grepioni, M. R. Chierotti, R. Gobetto and L. Pellegrino, *CrystEngComm*, 2010, **12**, 3534-3536.
[56] R. Liantonio, P. Metrangolo, T. Pilati, G. Resnati and A. Stevenazzi, *Cryst. Growth Des.*, 2003, **3**, 799-803.
[57] (a) D. Braga, F. Grepioni, L. Maini, S. Prosperi, R. Gobetto and M. R. Chierotti, *Chem. Commun.*, 2010, **46**, 7715-7717; (b) C. Butterhof, K. Barwinkel, J. Senker and J. Breu, *CrystEngComm*, 2012, **14**, 6744-6749; (c) D. Braga, F. Grepioni, L. Maini, D. Capucci, S. Nanna, J. Wouters, L. Aerts and L. Quere, *Chem. Commun.*, 2012, **48**, 8219-8221.
[58] J. R. Patel, R. A. Carlton, T. E. Needham, C. O. Chichester and F. G. Vogt, *Int. J. Pharm.*, 2012, **436**, 685-706.
[59] F. G. Vogt, J. S. Clawson, M. Strohmeier, A. J. Edwards, T. N. Pham and S. A. Watson, *Cryst. Growth Des.*, 2009, **9**, 921-937.
[60] D. Braga, L. Chelazzi, F. Grepioni, E. Dichiarante, M. R. Chierotti and R. Gobetto, *Cryst. Growth Des.*, 2013 in press
[61] S. Ando, J. Kikuchi, Y. Fujimura, Y. Ida, K. Higashi, K. Moribe and K. Yamamoto, *J. Pharm. Sci.*, 2012, **101**, 3214-3221.
[62] M. Khan, V. Enkelmann and G. Brunklaus, *J. Am. Chem. Soc.*, 2010, **132**, 5254-5263.
[63] F. G. Vogt, J. A. Vena, M. Chavda, J. S. Clawson, M. Strohmeier and M. E. Barnett, *J. Mol. Struct*., 2009, **932**, 16-30.
[64] A. S. Tatton, T. N. Pham, F. G. Vogt, D. Iuga, A. J. Edwards and S.P. Brown, *Mol. Pharm.*, 2013, **10**, 999-1007.
[65] K. Maruyoshi, D. Iuga, O. N. Antzutkin, A. Alhalaweh, S. P. Velaga and S. P. Brown, *Chem. Commun.*, 2012, **48**, 10844-10846.
[66] A. Lesage, D. Sakellariou, S. Steuernagel and L. Emsley, *J. Am. Chem. Soc.*, 1998, **120**, 13194-13201.
[67] D. Braga, G. Palladino, M. Polito, K. Rubini, F. Grepioni, M. R. Chierotti and R. Gobetto, *Chem. Eur. J.*, 2008, **14**, 10149-10159.
[68] M. Khan, V. Enkelmann and G. Brunklaus, *CrystEngComm*, 2011, **13**, 3213-3223.
[69] V. E. Zorin, S. P. Brown, P. Hodgkinson, *J. Chem. Phys.*, 2006, **125**, 144508.